Chapter 2

METAL PHYSICS

2.0.1 Electron focusing in Bi, Ag, W and Sb

If perfect metal crystals are cooled down to low temperatures T, the electronic mean free path l^* can acquire values in the mm-range, so ballistic transport through macroscopic samples is possible. If nonequilibrium carriers are thermoelectrically sent out from a small source (realized by local heating) at one surface of the sample they generate a current distribution in some distance $d < l^*$, which is characteristic of the materials band structure. A Cu point contact (PC) placed at the opposite surface, the collector (C), may be used for carrier detection.

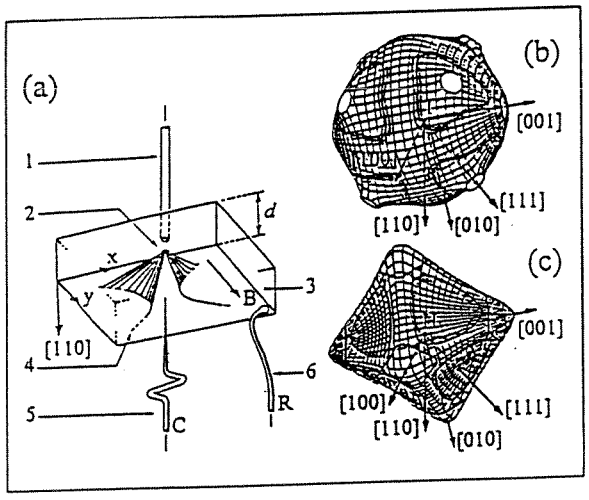

Figure 2.1: *(a) Scheme of the setup. See text for explanation, (b) and (c) Fermi surfaces of Ag and W (only hole octahedron). Numbers are explained in text.*

The direction of motion of an electron is given by its group velocity $\mathbf{v}_{gr} = \hbar^{-1}\nabla_k E(\mathbf{k})$. The Fermi surface (FS) is a surface of constant energy E_F, so $\mathbf{v}_{gr}$ is always perpendicular to the FS for carriers at the FS. The carrier current is enhanced in directions associated with regions of small gaussian curvature of the $(E(\mathbf{k}) = const)$ surfaces. If the gaussian curvature vanishes completely for some wavevector $\mathbf{k}$, all group velocities $\mathbf{v}_{gr}$ for neighbouring $\mathbf{k}$-states are parallel. This results in singularities in the current in the corresponding $\mathbf{v}_{gr}$- directions. We call the occurrence of such singularities or caustics *electronfocusing* (EF) in analogy to phonon focusing (PF).

The samples are thin plates cut from single crystals to slabs of $d \approx 2$ mm thickness. d was reduced to $\approx 0.1...0.5$ mm by electrochemical polishing or etching, thus $d \approx l^*$. The beam of a 30 mW Ar-laser is coupled into an optical fibre ((1) in figure 2.1 (a)). Its end is brought close to the upper surface of the sample (3). An area of $(\approx 20\mu\text{m})^2$ (hot spot) is illuminated with ≈ 3 mW (2). All experiments are performed in immersion in liquid ^{4}He at 1.5 K. To record an EF pattern, the hot spot is scanned across the upper sample surface by a cryogenic scanner (see "Versatile Threedimensional Cryogenic Micropositioning Device", this issue and Ref.[1]), which is equivalent to a fixed hot spot and a scanning C for a homogenous sample. The voltage V_C between C (5), which is spot welded to the lower surface, and a reference contact R on a sample edge (6) is recorded as a function of the fibre position.

EF patterns (4) For Bi, Ag, W and Sb are shown in figure 2.2. The EF pattern of Bismuth (Refs.[2],[3]) results from the three extremely streched electron ellipsoids, which can be approximated by cylinders inclined by 6°. In the planes perpendicular to the cylinder axis a strong current enhancement (producing the bright lines) can be found. The dark struc-

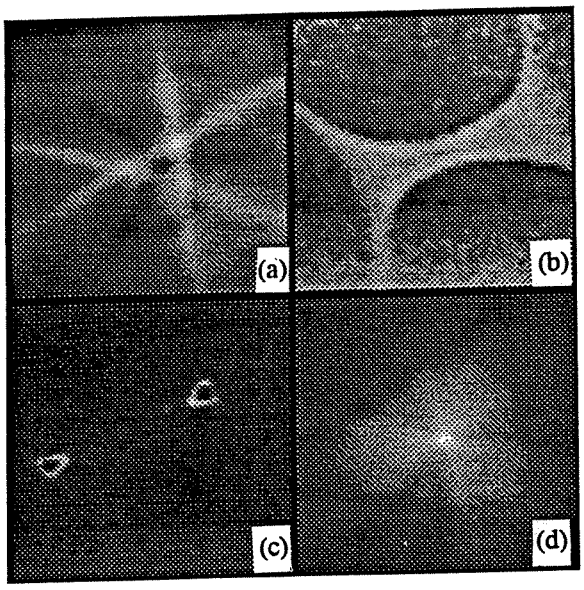

Figure 2.2: *Electron focusing patterns of (a) Bi (c-face), (b) Ag (110-face) , (c) W (110-face) and (d) Sb (c-face). V_C is shown in gray scale as a function of the fibre position.*

ture results from phonons. The EF pattern of Ag shows two bright electron caustics enclosing a bright field. They are generated by states near the necks of the Fermi Surface outlined by the shading in figure 2.1 (b). The dark rims stem from electrons at $E < E_F$ moving from occupied states in the bulk into empty states in the hot spot. In W the two bright triangular rings are obviously caused by states on the triangular faces of the hole octahedron shown in figure 2.1 (c). Because of its complex FS the origin of the EF-pattern in Sb is not yet understood.

For the first time a focusing of carriers along directions associated with regions on the FS with small (Bi, Sb?) and zero (Ag,W) gaussian curvature is clearly demonstrated. From the comparison of the experimental data with calculated EF patterns (not shown here) one can conclude, that electrons with $E = E_F$ produce the dominant contribution to the detector signal V_C. This allows to check the validity of FS- and band structure–models. The B-field dependence of the caustics furnishes supplementary information. Once fully understood, experiments of this kind will offer the unique possibility of k-resolved studies of virtually all band structure related features, the electronic dispersion of the medium playing the role of a spectrometer.

[1] J.Heil et al., Rev. Sci. Instrum. **67** (1), (1996)
[2] J.Heil et al., Phys. Rev. Lett. **74**, 146 (1995)
[3] M.Primke et al., accepted for publication in Physica B

J.Heil, M.Primke, A.Böhm, P.Wyder
H.Bender, E.Schönherr, H.Wendel (MPI-FKF, Stuttgart, Germany)
J.Major, P.Keppler (MPI-FMF, Stuttgart, Germany)
B.Wolf (University of Frankfurt, Germany)
P.Grosse (University of Aachen, Germany)

2.0.2 The Kondo–effect in high magnetic fields in small metallic contacts

In recent years, size effects in Kondo and spin–glass phenomena have attracted much attention and have become a higly controversial issue. The experiments mainly employ thin, narrow films to test the theoretical conjecture that, for length scales below a certain Kondo radius $R_c = \hbar v_F / 2\pi k_B T_K$ ($\simeq 1$ μm for Kondo temperature $T_K = 1$ K and typical Fermi velocity v_F), the Kondo scattering will be reduced. At present there is no overall agreement regarding this conjecture.

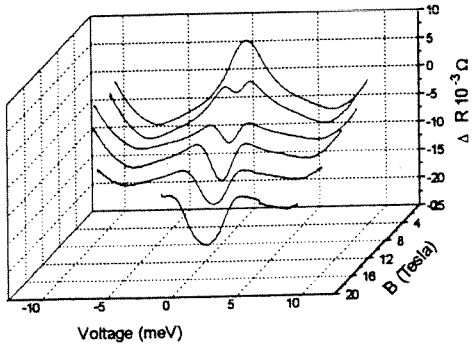

Figure 2.3: *The differential resistance of a break-junction with a Cu- 0.08 at % Mn alloy at 1.5 K as function of the applied voltage for magnetic fields from 0 to 20 with 4-T intervals. Contact resistance 1.1 Ω.*

If two metals are brought in contact and the diameter of the constriction is comparable to the electron

the magnet site and had to be removed after each magnet–time. To avoid the time consuming line–up, in the new setup all lasers are placed in the laboratory above the magnet M9. A new insert was constructed, which allows the work in a Helium bath cryostat where ESE measurements can be done at temperatures down to 1.6 Kelvin.

Due to problems with M9 the required field of 22 Tesla was not available and the testing of the new setup will be delayed.

[1] C.Kutter, H.P.Moll, H.van Tol, H.Zuckermann, J.C.Maan, P.Wyder, Phys. Rev. Lett. **74**, 2925 (1995)

H.P.Moll, H.van Tol, G.Rikken, P.Wyder

6.3.5 Versatile three–dimensional cryogenic micropositioning device

We present a versatile mechanical micropositioning unit offering positioning in three–dimensions along three orthogonal directions. Its design is compact and simple and its operation is intuitive and straightforward. It is entirely constructed from nonmagnetic materials, thus it can be used in magnetic fields and in cryogenic environments. It was originally designed for point contact experiments but it may be useful in any application, where movements of samples and/or probes are needed and in scanned probe microscope–techniques.

Figure 6.8 shows a schematic representation of the construction. The key element is a three–dimensional parallelogram composed of 5 leaf springs and a wire cross. To actuate the probe support to a desired position, three brass screws are used, each associated to the motion in x-, y- and z-direction respectively.

Figure 6.9 shows a setup composed of two scanners like those presented in figure 6.8 fitted into one another and displaced some mm from each other. We used this setup to perform so called electron focusing experiments (see "electron focusing in Bi, Ag, W and Sb", this issue and Ref.[1]).

Positions within a volume of roughly $(2\ \mathrm{mm})^3$ are attainable. The mechanism can be scaled up (or down) to have access to larger (or smaller) scan ranges. The following characteristics are derived from the measurements: the sensivity is about 700 μm /screw revolution in x- and y-direction and

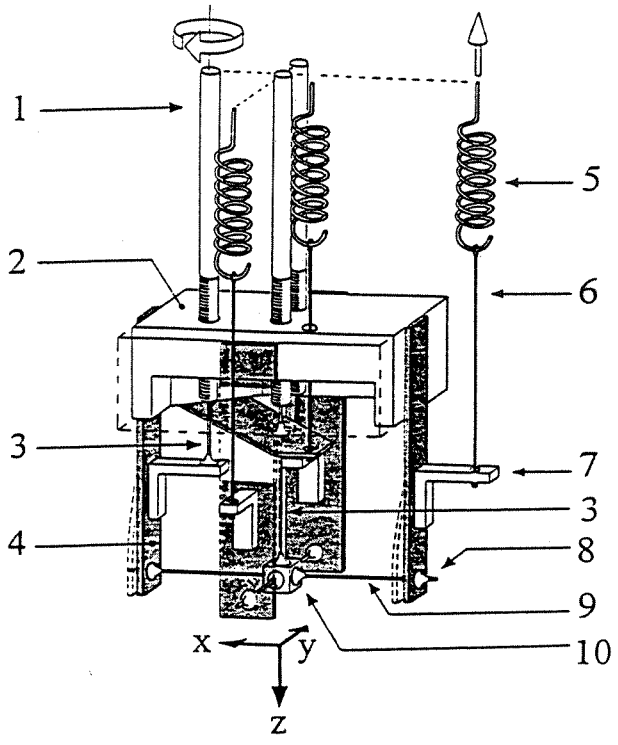

Figure 6.8: *Schematic representation of the scanner mechanics. (1) brass screw (M3 × 350 μm), (2) base structure made from brass (partly cut away), (3) bronze wire (0.6 mm diameter), (4) bronze leaf spring (0.3 mm thickness), (5) helical spring made from bronze wire (0.6 mm diameter), (6) string from artificial silk, (7) brass lever, (8) soft soldering, (9) bronze wire (0.4 mm diameter), (10) probe support. Turning the x-screw results in a deformation of the structure indicated by the dashed lines (figure from Ref.[1]).*

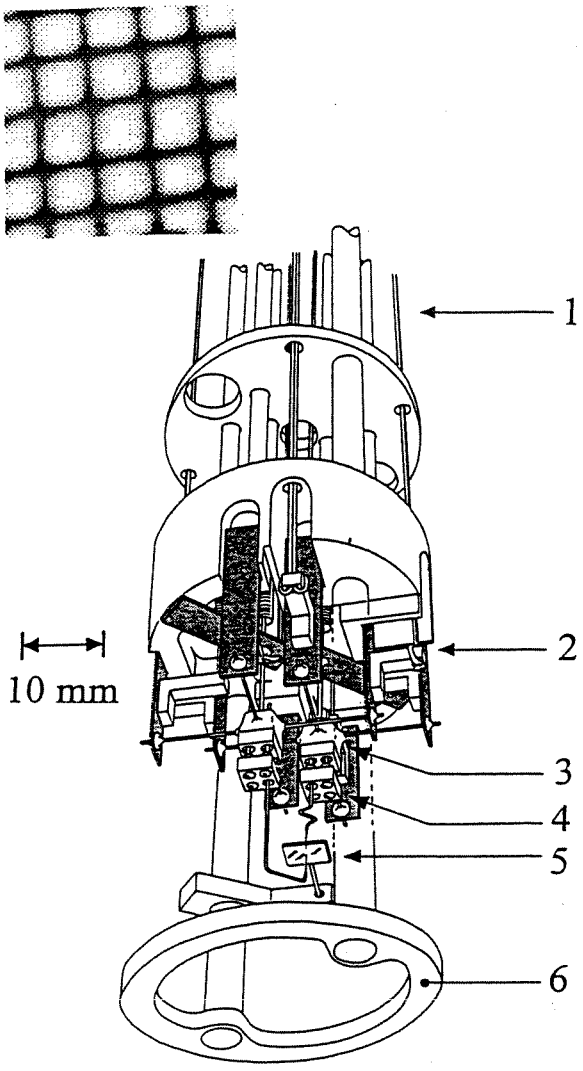

Figure 6.9: *Setup for an electron focusing experiment. Two scanners of the kind shown in figure 6.8 are mounted together (1) control-tubes and strings to the springs, (2) scanner, (3) probe supports (4) IC-pin connectors with point contacts plugged into the supports, (5) sample, (6) ring for mechanical protection. Inset : Calibration measurement performed on a Cu-mesh with a lattice constant of 60 μm : frame (400×320) steps corresponding to (265μm)^2, (80×64) data (figure from Ref.[1]).*

350 μm in z-direction. The resolution is better than 1 μm ; the reproducibility in positioning is at least comparable to the resolution. 1/1000 (or even less) screw revolution is easily controlable in the experiment. The deviations from linearity are smaller than 10 % for the whole working range and the deviation from orthogonality is smaller than 3°. An example for a calibration measurement is shown in the inset of figure 6.9.

[1] J.Heil et al., Rev. Sci.Instrum. **67**, (1), (1996)

J.Heil, M.Primke, A.Böhm, P.Wyder, J.Dettinger, H.Dresler, R.Pankow, J.Spitznagel

6.3.6 New dilution refrigerator for polarized luminescence studies in high magnetic fields

The optical study of a two–dimensional electron gas in the Quantum Hall regime requires very low temperatures (T<300 mK), high magnetic fields (at least 20 T) and measurements of spectra in circular polarization. A new dilution refrigerator has been developed with a central optical tube (light pipe), a lens on its bottom allowing for focusing the laser beam onto the sample and an optical bench with polarizing filters (P) mounted on the top of the system which has a total length of 2.20 m, a diameter of 30 mm and is inserted directly into an existing cryostat which can be used for any resistive magnet of the LCMI.

The optical bench contains two microscopical objectives for making parallel the incoming laser beam transmitted by an optical fibre (no. 1) and for focusing the luminescence beam coming back from the sample to a second fibre (no. 2) which connects the experiment to an OMA spectrometer (distance from the magnet up to 40 m). Both beams are separated by a beamsplitter. The exciting beam enters the 8.5 mm hollow light pipe through an optical window and is focused by a lens (f $\approx$ 35 mm) onto the sample mounted in the ^{3}He-^{4}He mixing chamber. The optical tube and its lens are vertically mobile which enables to optimize the focal distance according to sample thickness and temperature. Before entering the second optical fibre the outgoing beam passes a circular polarizer which allows to compare directly left - and right–hand polarized spectra (σ^+ and σ^-) for a given magnetic field.